



Fermilab

Accelerator Physics Center

Update on DPA calculations

Sergei Striganov

Joint HiLumi-LARP Meeting & 24th LARP
Collaboration Meeting

Fermilab

May 11, 2015

OUTLINE

- DPA calculation in NRT model
- Calculations of NIEL & DPA using different models of Coulomb scattering
- Molecular Dynamics corrections to NRT model
- Comparison with experimental data and IOTA
- Conclusion

Atomic displacement cross section

Displacement cross section is reference measure used to characterize and compare the radiation damage induced by neutrons and charged particles in crystalline materials. To evaluate number of displaced atoms Norgett, Torrens and Robinson proposed in 1975 a standard (so-called NRT-dpa), which has been widely used from that time.

Nowadays this formulation is recognized as suffering from some limitations: it is not applicable for compound materials, does not account for recombination of atoms during cascade, cannot be directly validated and has no uncertainties as evaluated cross sections usually have now.

Upgrading of dpa-standard means inclusion of results of Molecular Dynamics (MD), Binary Collision Approximation (BCA) for primary radiation defects, which survive after relaxations of Primary Knock-on Atom (PKA) cascade.

Atomic displacement cross section and NIEL

Atomic displacement cross section

$$\sigma_d = \sum_r \int_{E_d}^{T_r^{\max}} \frac{d\sigma(E, Z_t, A_t, Z_r, A_r)}{dT_r} N_d(T_r, Z_t, A_t, Z_r, A_r) dT_r$$

N_d - number of stable defects produced, E_d - displacement threshold, $d\sigma/dT_r$ - recoil fragment energy (T_r) distribution.

Non-ionizing energy loss (NIEL)

$$\frac{dE}{dx_{ni}} = N \sum_r \int_{E_d}^{T_r^{\max}} \frac{d\sigma(E, Z_t, A_t, Z_r, A_r)}{dT_r} T_d(T_r, Z_t, A_t, Z_r, A_r) dT_r$$

N - number of atoms per unit volume, T_d - damage energy = total energy lost in non-ionizing process (atomic motion)

**NRT - "standard" model:
how to calculate number of Frenkel pairs and damage energy**

M.J. Norgett, M.T. Robinson, I.M. Torrens Nucl. Eng. Des 33, 50 (1975)

$$N_d = \frac{0.8}{2E_d} T_d$$

$$T_d = \frac{T_r}{1 + k(Z_t, A_t, Z_r, A_r)g(T_r, Z_t, A_t, Z_r, A_r)}$$

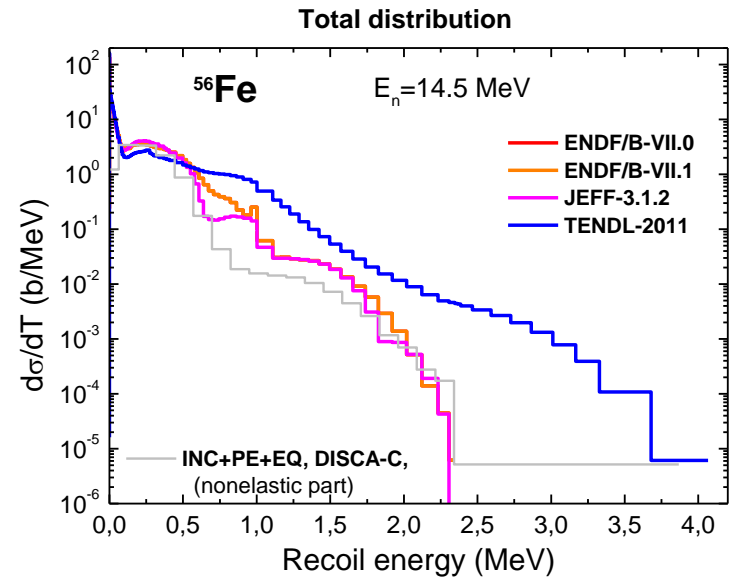
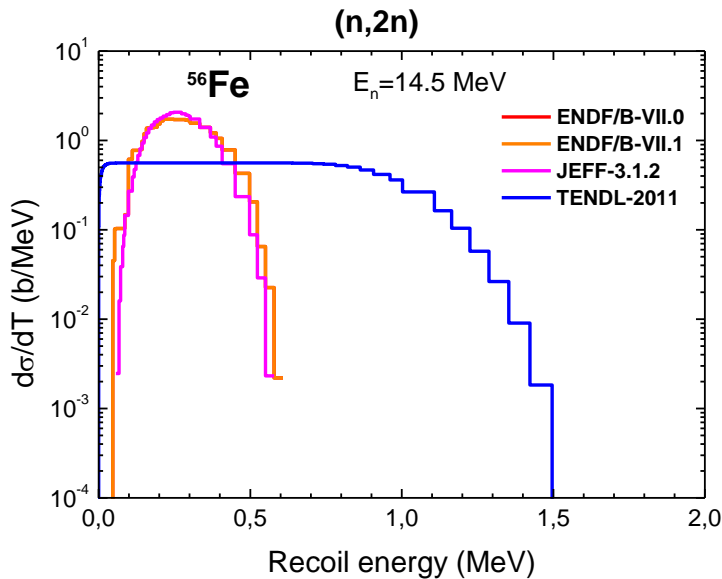
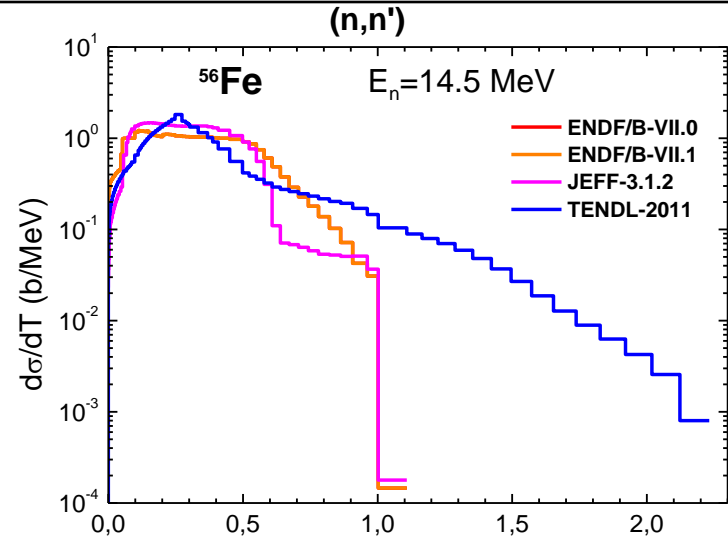
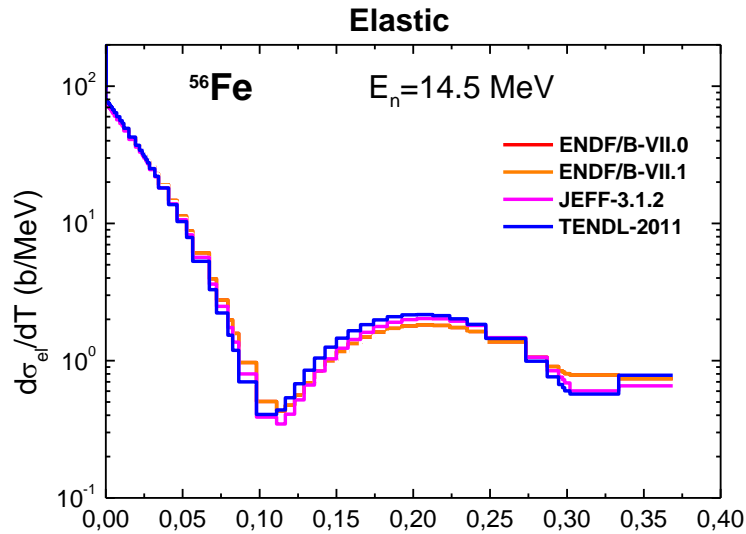
T_r, Z_r, A_r - recoil fragment energy=primary knock-on (PKA) energy, charge and atomic mass

Z_t, A_t - charge and atomic mass of irradiated material.

Nuclear physic (T_r, T_d) + solid state physics (N_d).

NRT-dpa was successfully applied to correlate data from many studies involving direct comparison from very different irradiation environments.

Recoil energy distributions



Models of Elastic Coulomb scattering

- At energies below 10 MeV, Coulomb interactions dominate the production of displaced atoms from their lattice sites
- For protons classical mechanics approach can be used at energies $< Z/10$ MeV
- Quantum-mechanical description of elastic scattering including a relativistic treatment is also available
- Classical and quantum mechanics provide similar results at energies $> Z/10$ MeV where relativistic and spin effects do not important

Models of Elastic Coulomb scattering-II

- **IOTA code** (Konobeyev et al), **NASA SEE** and **SET** programs (Jun et al) - energy-transfer differential cross section based on Lindhard, Nielsen, Scharff "Approximation method in classical scattering by screened coulomb field". This approach was applied to Tomas-Fermi potential. Reduced scattering cross section was obtained as a function of a single scattering parameter.
- At large momentum transfer this cross section has same behavior as Rutherford cross section - cross section for scattering on unscreened Coulomb potential

Models of Elastic Coulomb scattering-III

- **G4** code (Boschini et al) - Wentzel-Moliere treatment of single scattering

$$\frac{d\sigma^{WM}}{dT} = 2\pi \left(\frac{zZe^2}{\beta} \right)^2 \frac{1}{(T + p^2 \chi_a^2 / (2M))^2}$$

χ_a^2 - Moliere screening parameter. T , Z and M energy, charge and mass of recoil nuclei. z , p and β - charge, momentum and velocity of projectile

Models of Elastic Coulomb scattering-IV

MARS code - Wentzel-Moliere formula with spin correction and nuclear screening

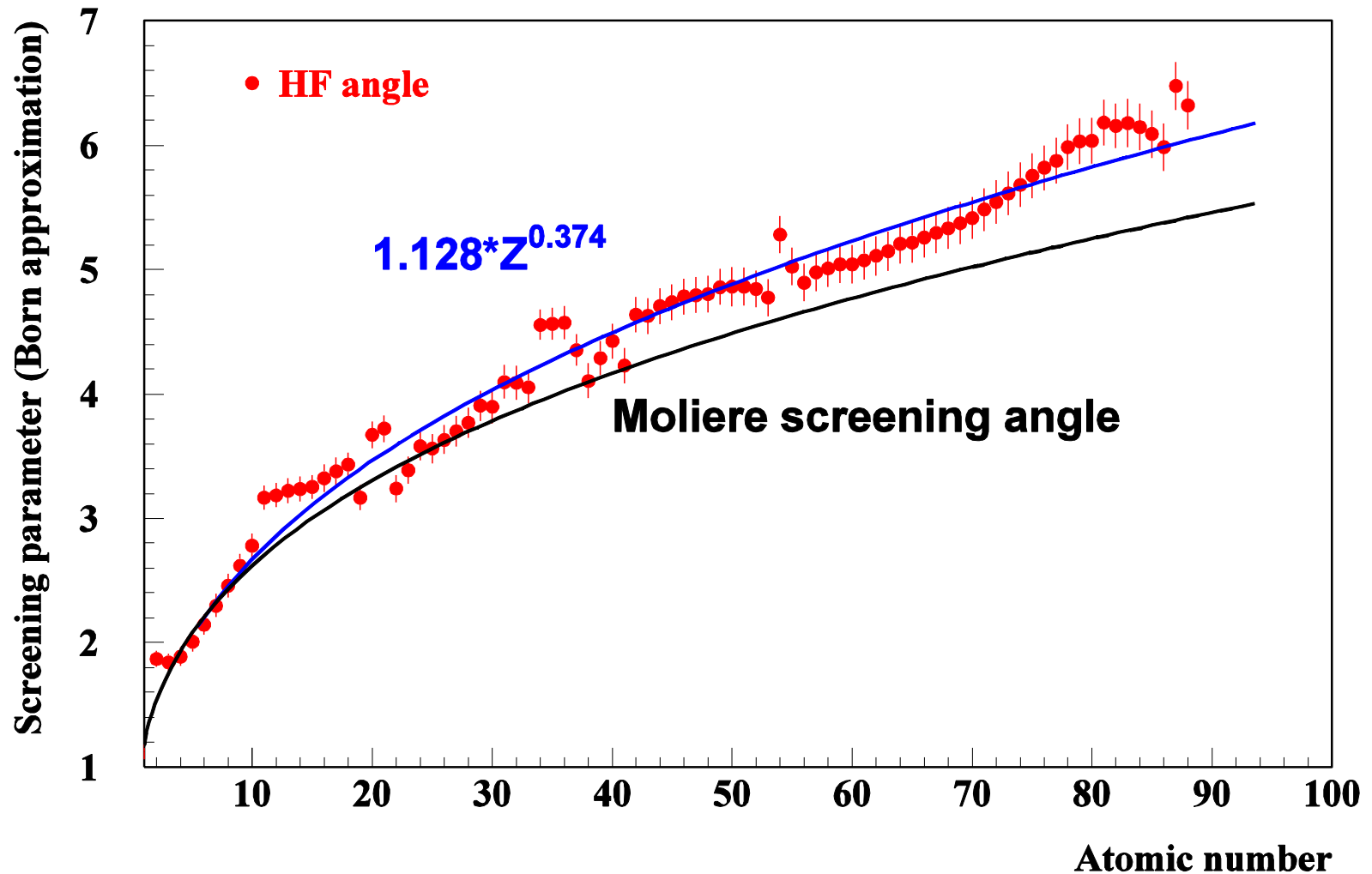
$$\frac{d\sigma}{dT} = \frac{d\sigma^{WM}}{dT} R_M(T) F_n(q)$$

R_M - Mott spin correction. F_n - nuclear form factor squared, q - momentum transfer.

Moliere calculated the screening angle using Thomas-Fermi model. Atomic screening of all nucleus is described using by 6 parameters only. Hartree-Fock approach takes into account individual properties of atoms—in particular, their shell structure.

Correction to Born approximation could be applied using different methods.

Screening parameter in Hartree-Fock model



Comparison with other calculations

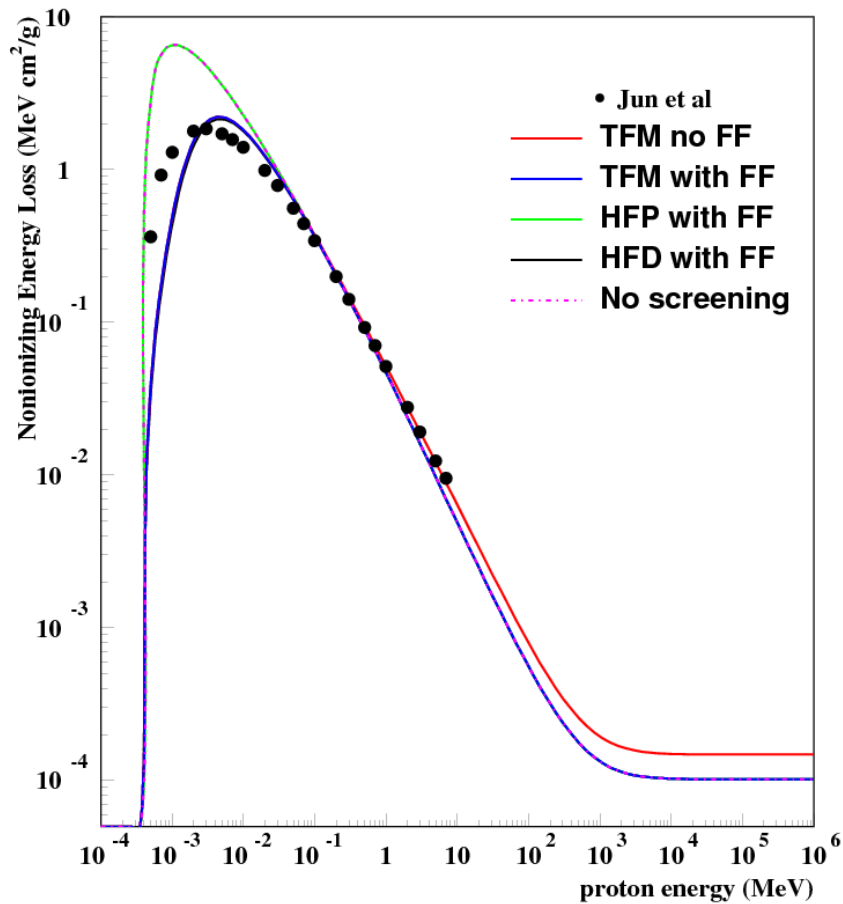
We are going to compare calculation Non-Ionizing Energy-Loss (NIEL) and DPA using:

- classical approach: **NASA team** - Jun et al and **IOTA code** - Konobeyev et al
- quantum-mechanics Tomas-Fermi-Moliere approach - **G4 team** - Boschini et al

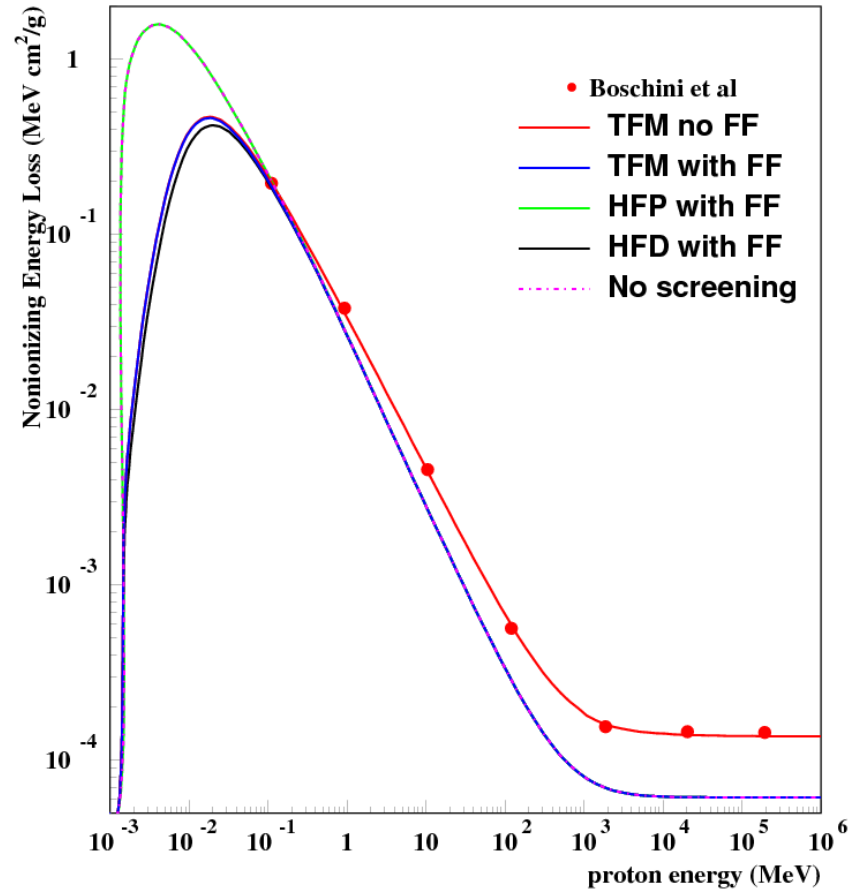
With our quantum-mechanics calculations:

- Tomas-Fermi-Moliere-Mott + nuclear screening - **TFM** Moliere screening parameter and **TFM(3)** Moliere from-factor
- Hartree-Fock-Penelope-Mott + nuclear screening - **HFP** Hartree-Fock screening parameter in Born approximation and **HFP(3)** HF from-factor. Penelopa "practical correction" at low energies
- Hartree-Fock-Moliere-Dubna-Mott + nuclear screening - **HFD** Hartree-Fock screening parameter in Born approximation and **HFD(3)** HF from-factor. Dubna Coulomb correction at ultrarelativistic energies. Moliere Coulomb correction at low energies.

Comparison with other calculation: NIEL

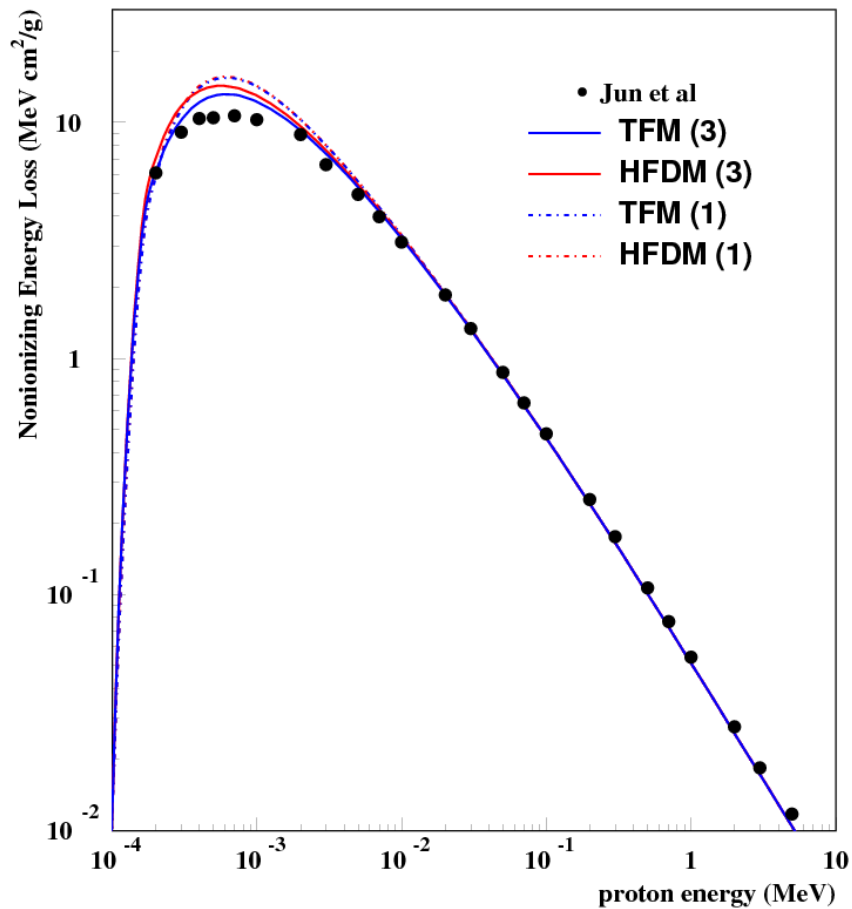


Proton NIEL for copper due the Coulomb scattering

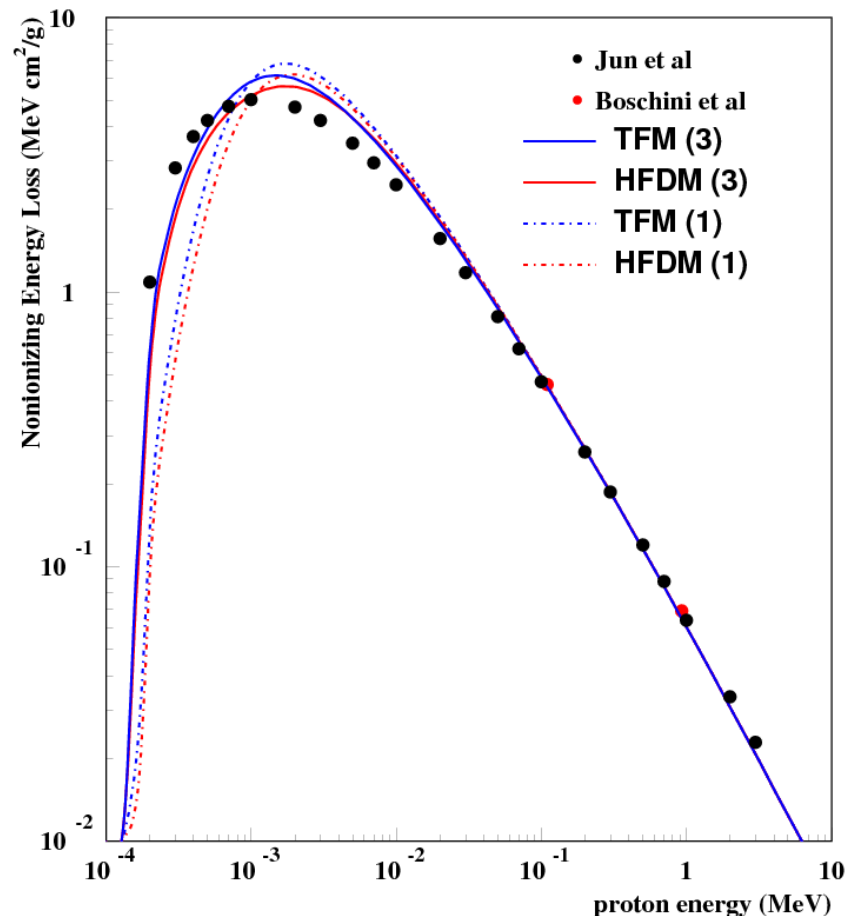


Proton NIEL for lead due the Coulomb scattering

Full form factor against Moliere approximation

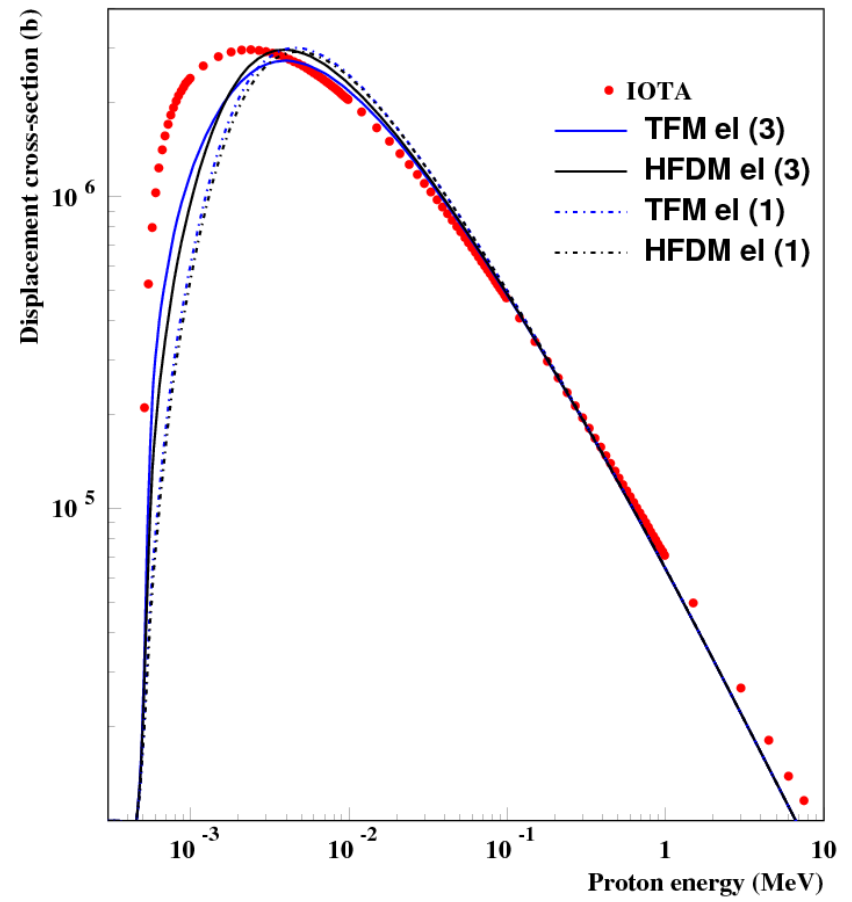
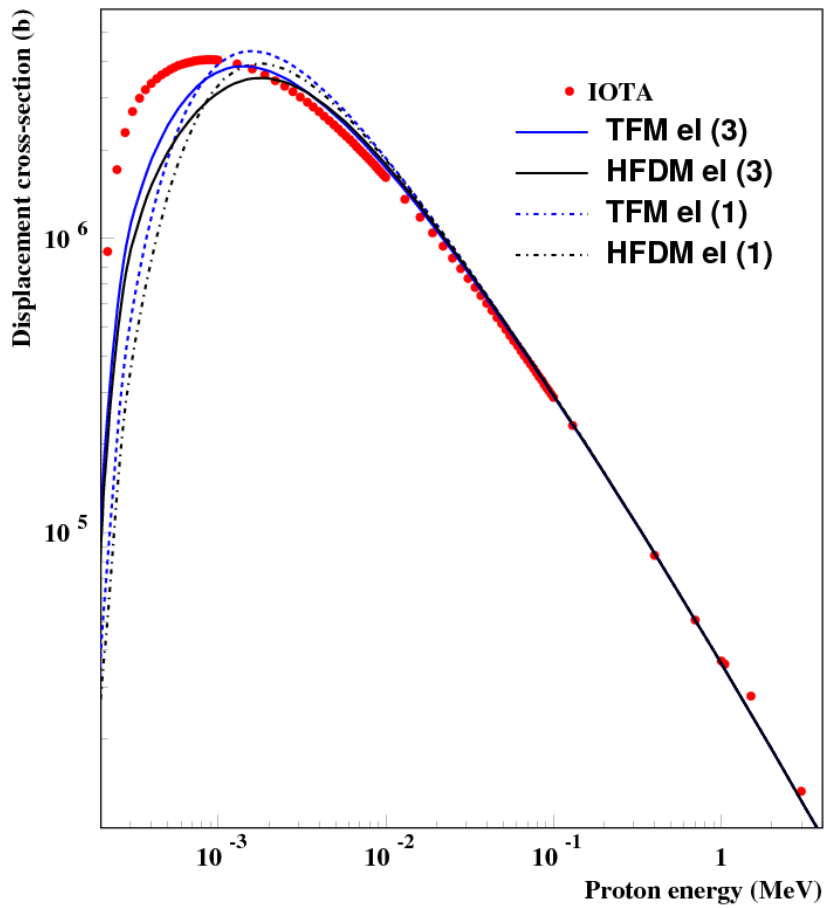


Proton NIEL for carbon due the Coulomb scattering



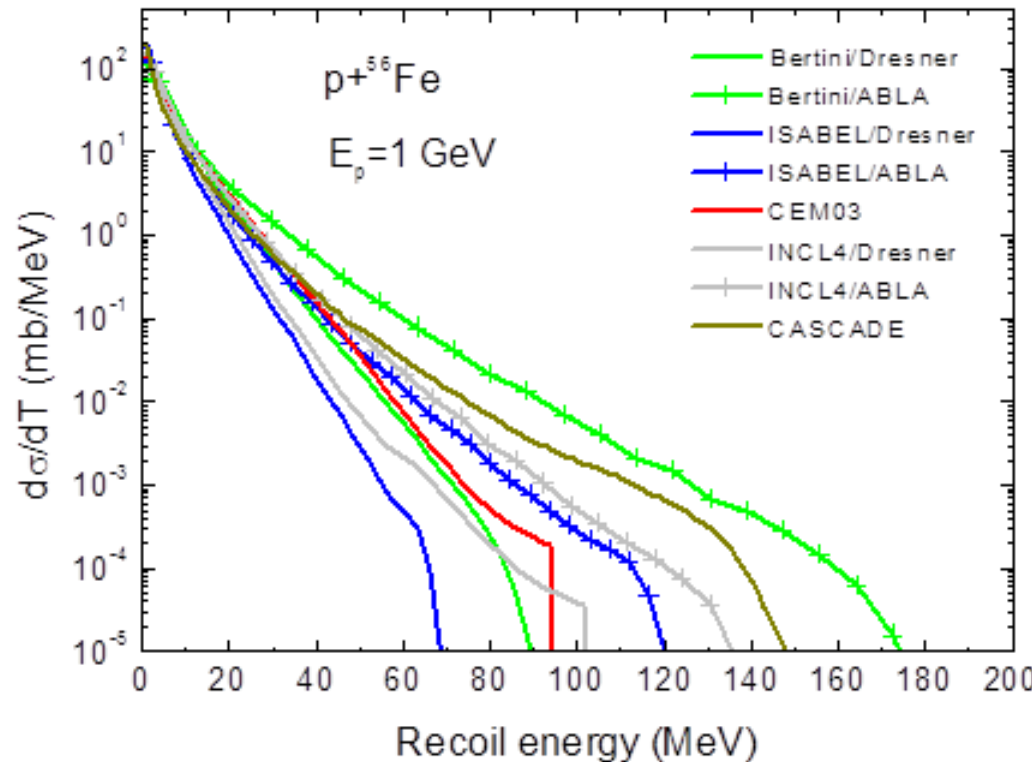
Proton NIEL for silicon due the Coulomb scattering

Full form factor against Moliere approximation

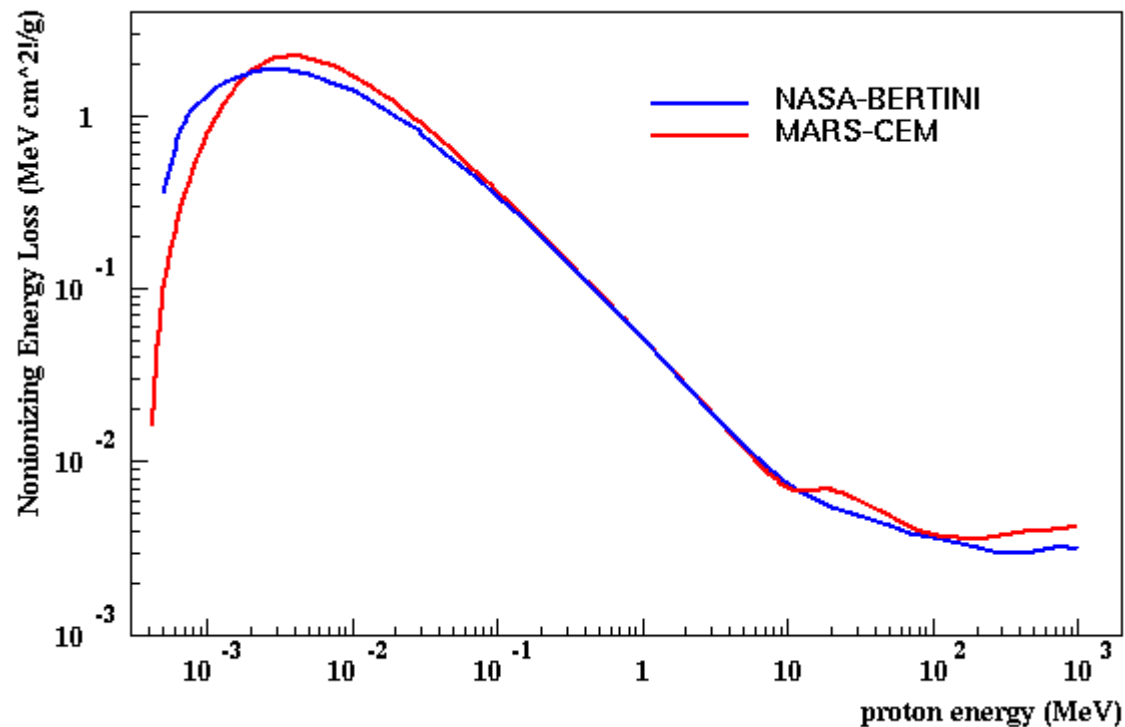


Models of inelastic interaction

To simulate primary knock-on energy (PKA) in inelastic interaction at energies lower few GeV intra-nuclear cascade following by pre-equilibrium and evaporation should be simulated. Dozens of model available on the market. At higher energies quark-gluon string models could be applied. Note, that displacement cross sections obtained with above models could be different up to 50%.

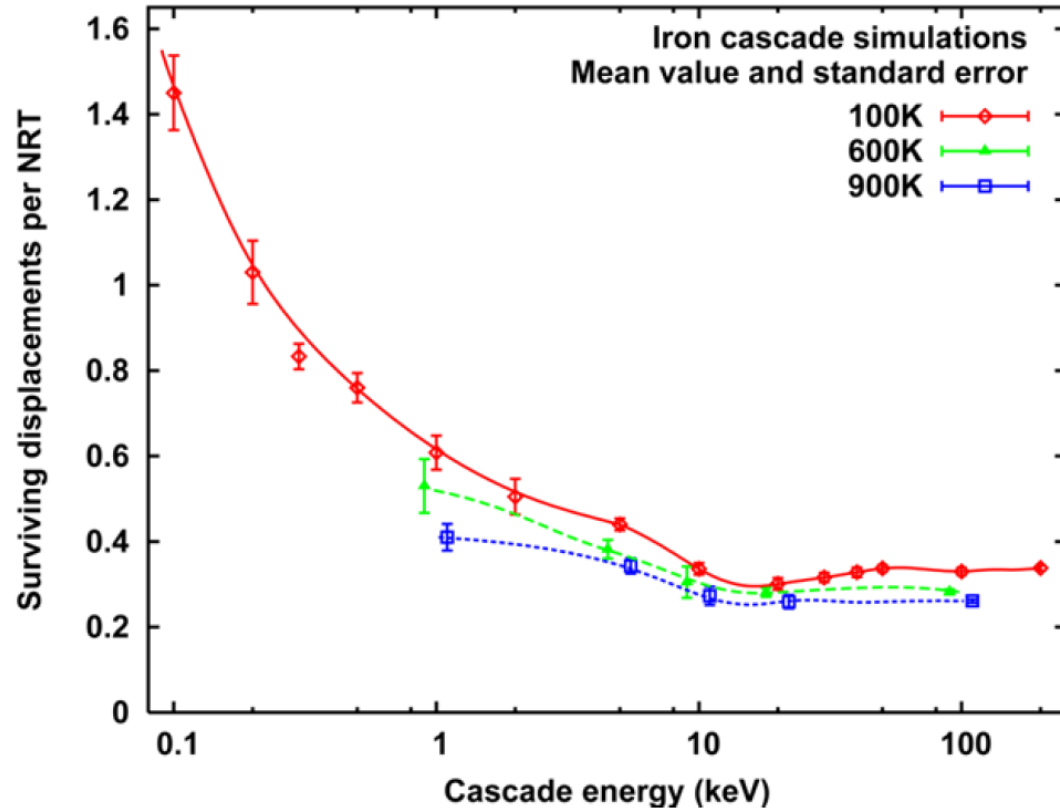


NIEL in copper - MARS vs NASA calculation



Direct calculation of atomic displacement

Modern computer capabilities and improved interatomic potentials have enabled molecular dynamics (MD) simulations to characterize point defect formation in atomic displacement cascade. Large MD cascade database with energies up to 200 keV and temperatures of 100-900K was created by Stoller. Number of stable displacement in MD simulation is about 30% of NRT above about 20 keV. This data are parametrized and using as correction to NRT in FLUKA and MARS.



Modified NRT equation for damage developed by OECD NEA primary damage group

It is well established that the damage in elemental metals is much smaller than value predicted by NRT equations.

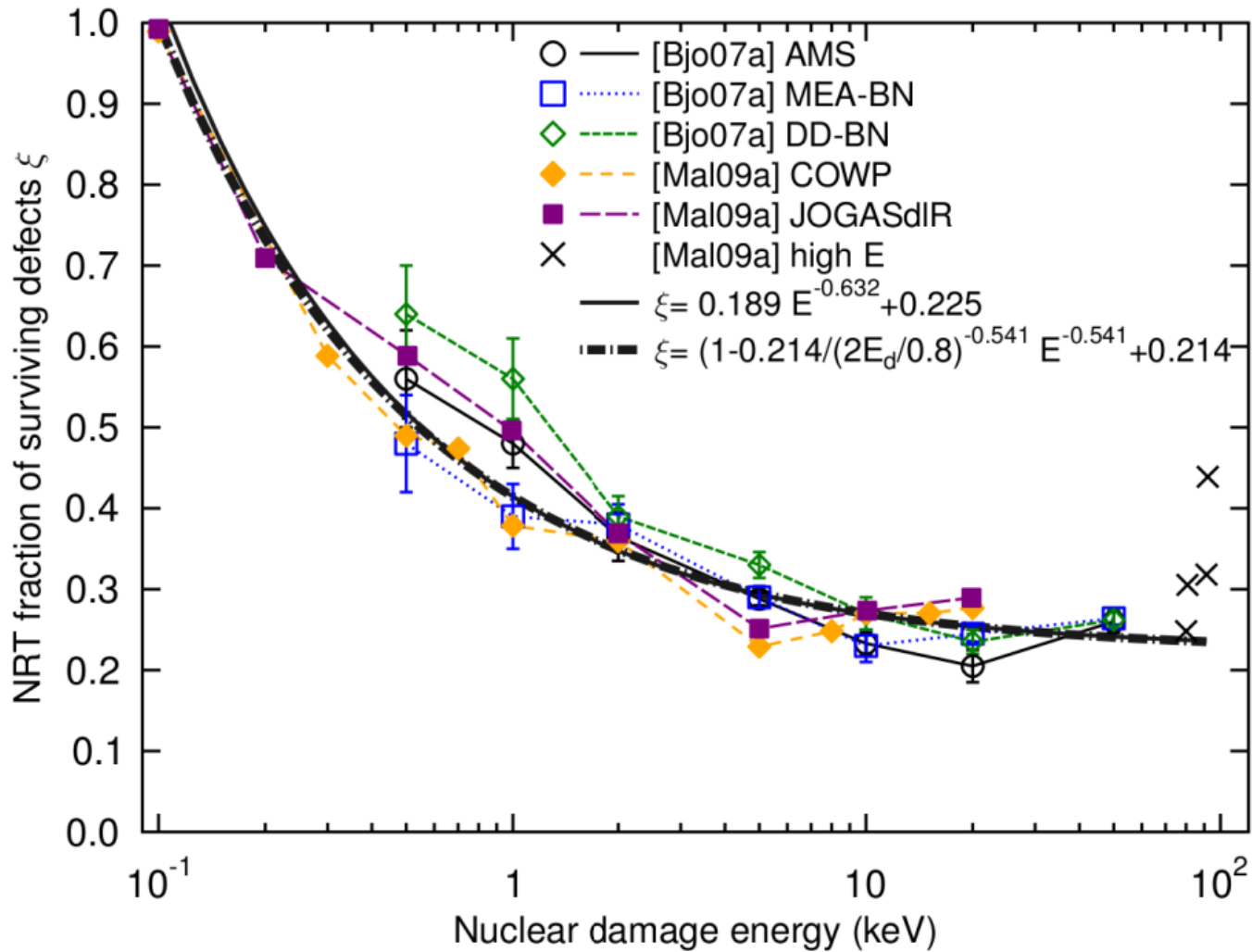
Nuclear Energy Agency primary damage group (Kai Nordlund et al) propose new damage formalism to calculate number of defects

$$N_d = \begin{cases} 0 & T_d < E_d \\ 1 & E_d < T_d < 2.5E_d \\ \frac{2.5T_d}{E_d} \xi(T_d) & 2.5E_d < T_d \end{cases}$$

Efficiency function $\xi(T)$

$$\xi(T) = 0.214 + 0.786 \times (2.5E_d / T)^{0.541}$$

Fit of the new damage function



Experimental data relevant to dpa calculations

Quantity	Projectile	Energy	Target	Reference
Displacement cross-section	p, d, ⁴ He, (electrons)	0.0005 to 20 MeV, (0.2 to 4 MeV)	Al, V, Fe, SS, Ni, Cu, Nb, Mo, Pd, Ag, Ta, W, Pt, Au	P. Jung, J. Nucl. Mater. 117, 70 (1983)
$\langle K_d \rangle$, $\langle \xi \rangle$	neutrons	reactor spectra	Mg, Al, K, Ti, V, Fe, SS, Co, Ni, Cu, Zn, Ga, Zr, Nb, Mo, Pd, Ag, Cd, Sn, Ta, W, Re, Pt, Au, Pb	C.H.M. Broeders et al, J. Nucl. Mater. 328, 197 (2004)

Experimental data relevant to dpa calculations-II

Quantity	Projectile	Energy	Target	Reference
Displacement cross-section	O, Ar, Kr, Xe, Pb, U	0.096 to 4.68 GeV	Fe (Ed = 25 eV)	A. Dunlop et al, <i>Nucl. Instr. Meth. B90, 330 (1994)</i>
Displacement cross-section	protons	1.1, 1.94 GeV	Cu, W	G.A. Greene et al, <i>AccApp ('03)</i>

Experimental data relevant to dpa calculations-III

Jung et al and Greene et al measured resistivity change due to proton, electron, light ion, fast and low energy neutron at low temperature and low doses. It is connected with displacement cross section σ_d

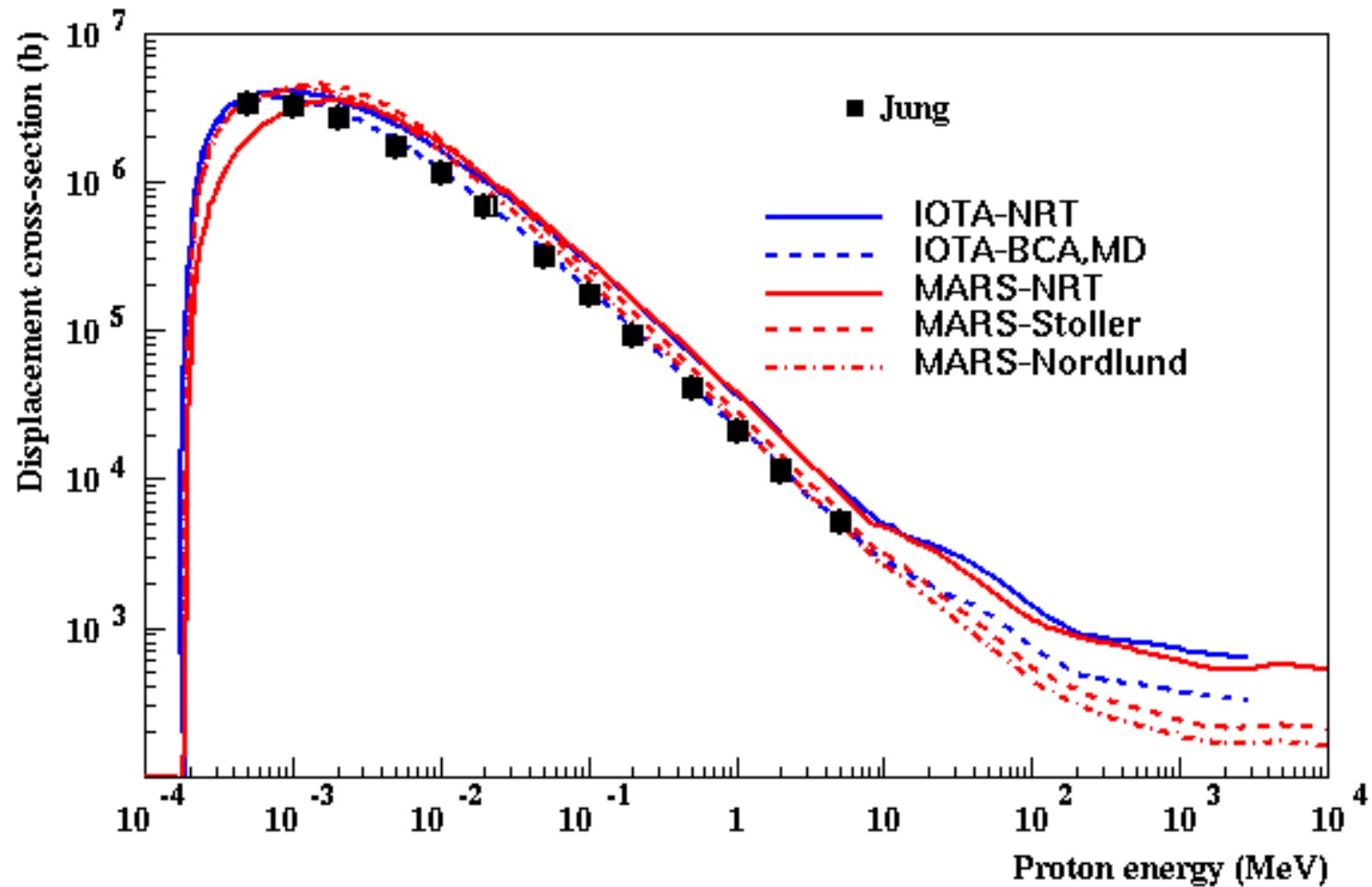
$$\Delta\rho_d(\Phi, E) = \Phi \sigma_d(E)\rho_F$$

ρ_F is resistivity per unit concentration of Frenkel defects. This constant cannot be calculated theoretically with sufficient precision. It is determined from measurements. Jung and Greene groups choose different ρ_F ($\mu\Omega\text{m/u.c.}$) for same material

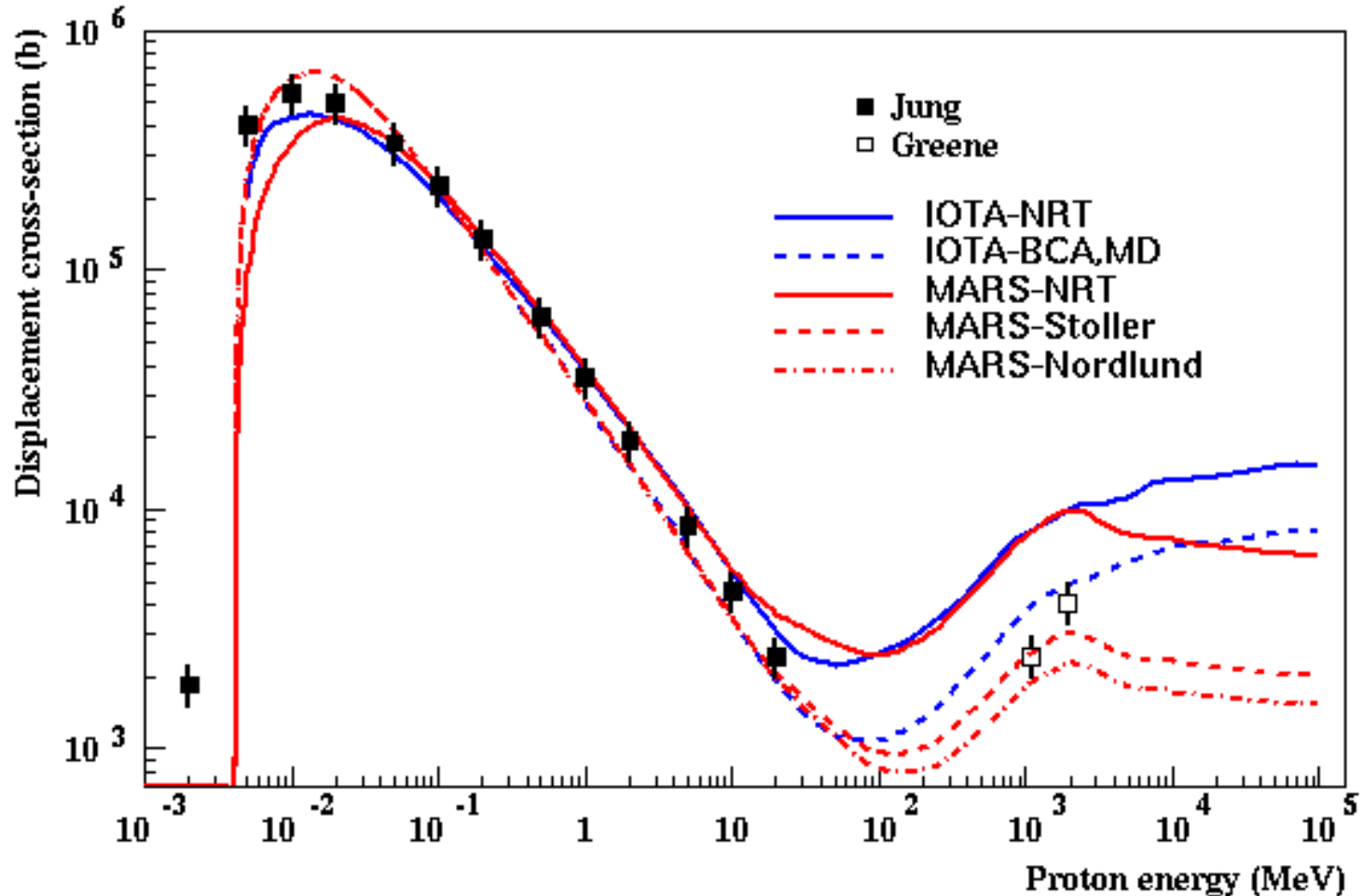
	Jung	Greene
Cu	2.5 +- 0.3	2
W	27 +- 6	14

Konobeev&Broeders&Fisher (IOTA) note that Greene choice seems questionable taking account later analysis.

Displacement cross section in aluminum: IOTA, MARS and experimental data



Displacement cross section in tungsten: IOTA, MARS and experimental data



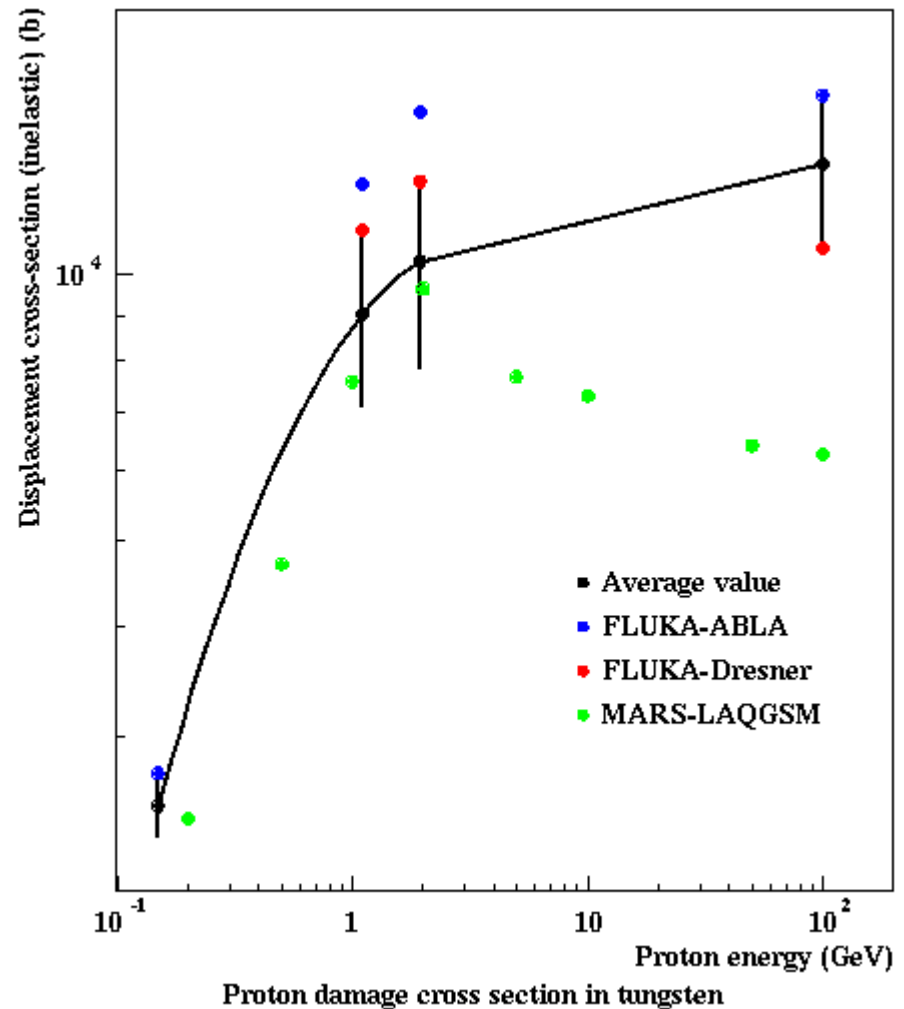
High energy rise of IOTA displacement cross section in tungsten is result of averaging

At energies lower than few GeV Iota team was using average value of cross sections obtained with 8 cascade codes.

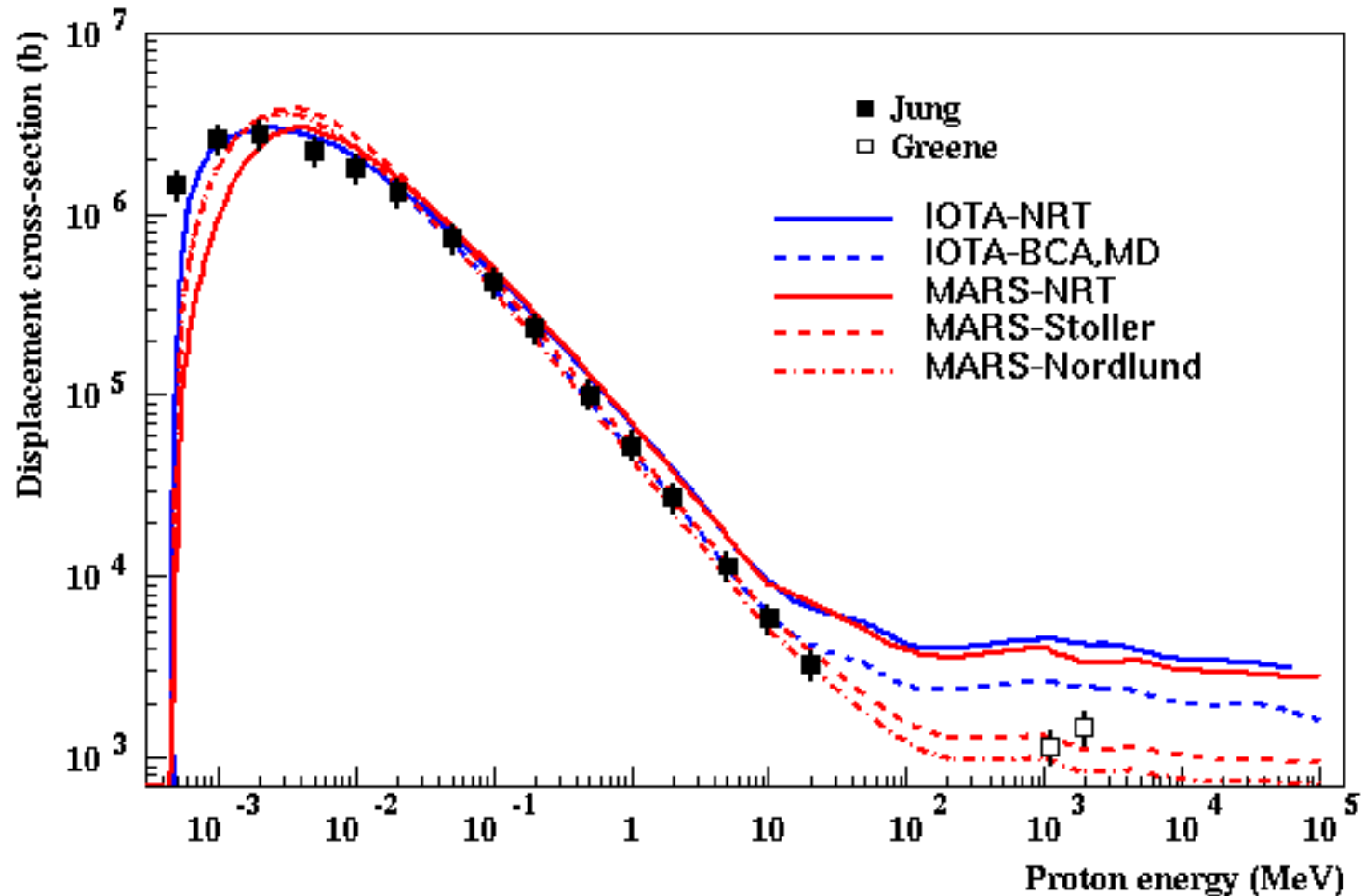
At high energy only 2 codes were available - FLUKA-ABLA and FLUKA-Dresner. So, high energy rise of average cross section appears because different sample of codes is used at low and high energies.

FLUKA-Dresner cross sections shows dependence on energy similar to MARS-LAQGSM.

FLUKA-ABLA cross sections shows few percents rise.

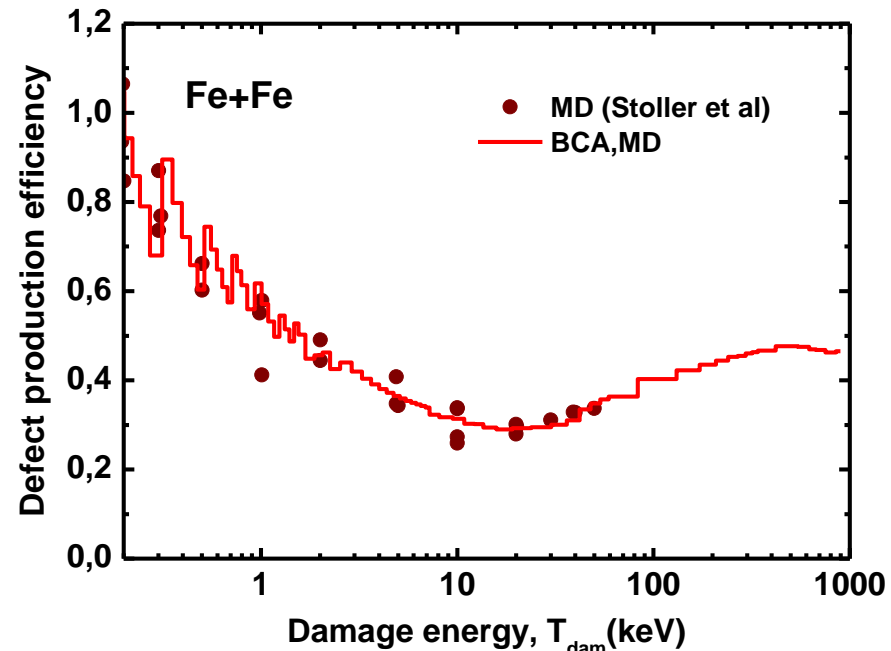
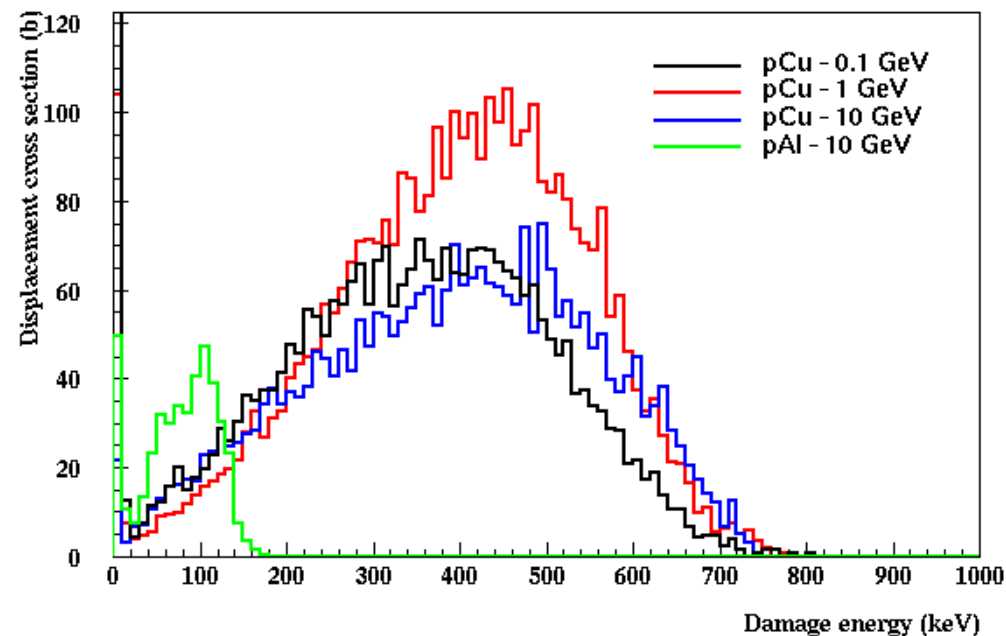


Displacement cross section in copper: IOTA, MARS and experimental data



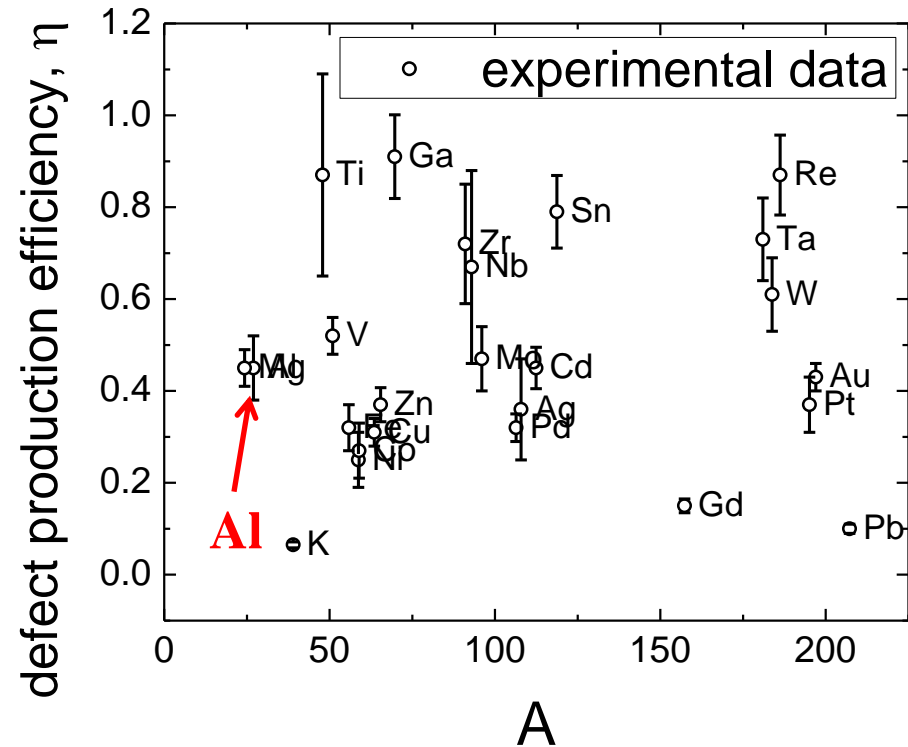
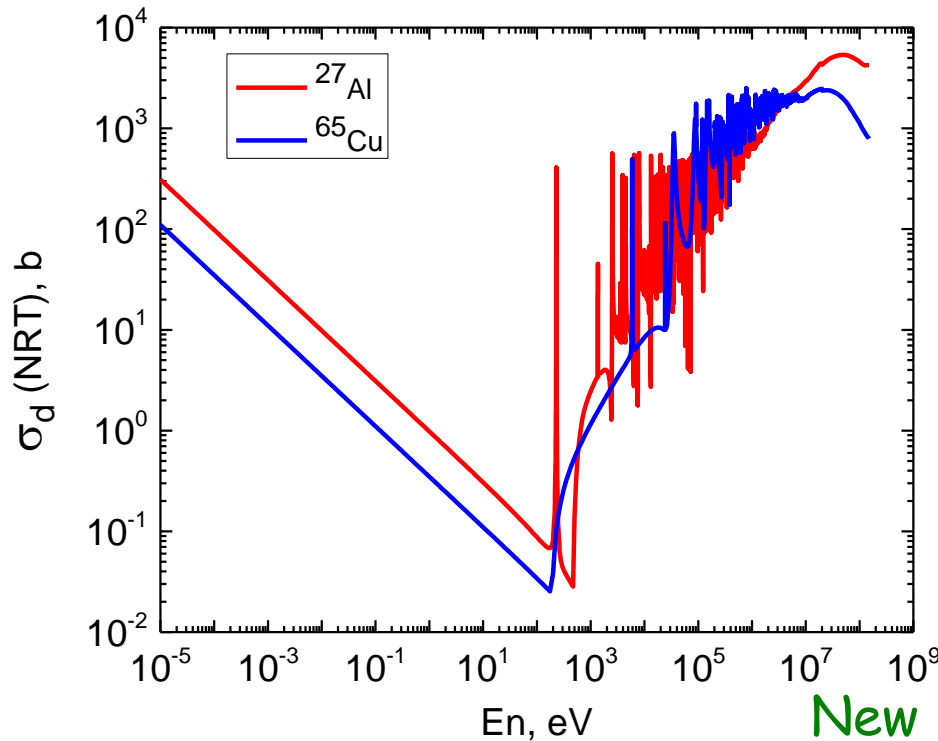
Why MARS post-NRT calculation of displacement x-section smaller MD-BCA result at high energies?

Stoller and Nortlund corrections to NRT based on MD simulation performed for damage energies lower 100 keV. Its become constant (0.3 and 0.21) at energies larger 100 keV. Damage energy in inelastic interaction is large. IOTA results were obtained in BCA&MD simulation. Defect production efficiency in this model at is 1.5-2 times then Stoller/Nortlund corrections at 100-1000 keV.



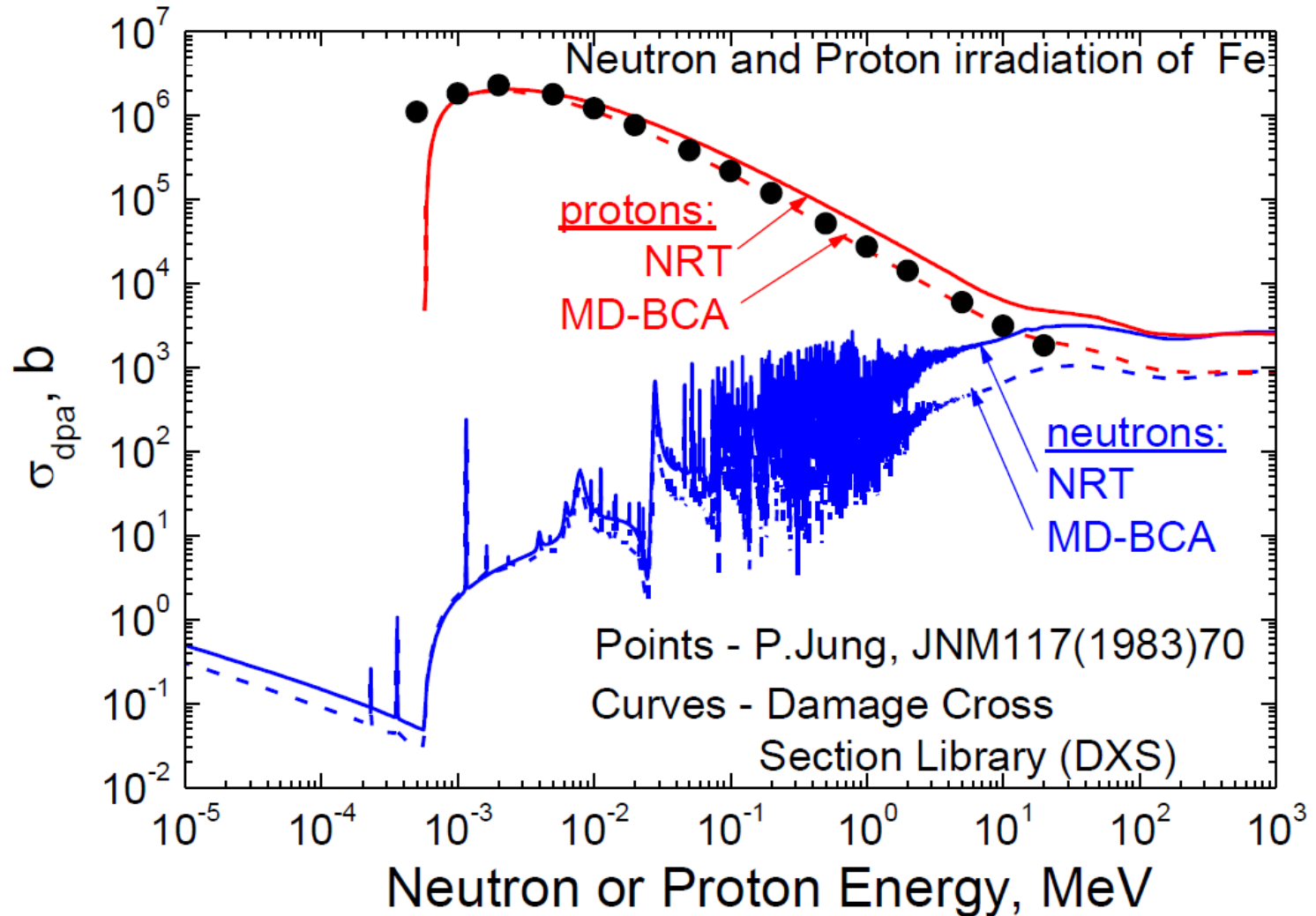
Medium- and Low-E Neutron DPA Model in MARS15

T = 4-6 K



For neutrons from 10^{-5} eV to 150 MeV: NJOY99+ENDF-VII database, for 393 nuclides. At T=4-6K, optional correction for experimental defect production efficiency η (Broeders, Konobeev, 2004), where η is a ratio of a number of single interstitial atom vacancy pairs (Frenkel pairs) produced in a material to the number of defects calculated using NRT model

DPA cross section in iron



Conclusion

Atomic displacement cross sections obtained using "standard" NRT model and different approaches (IOTA, NASA, G4, MARS) are in close agreement except high Z materials and high energies (>10 GeV)

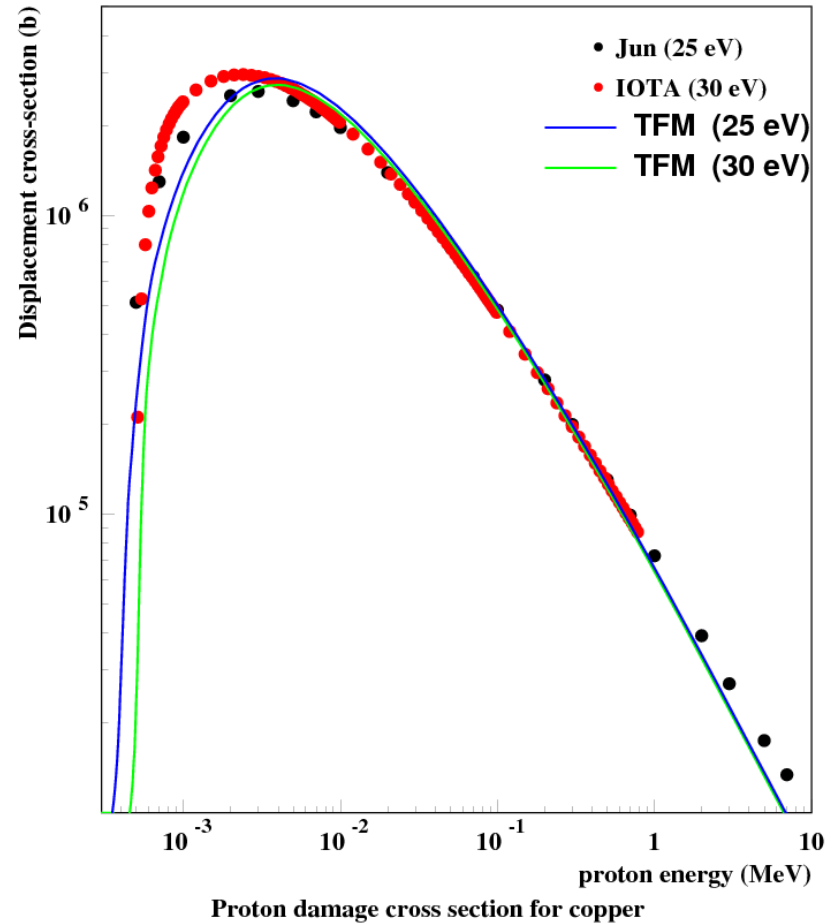
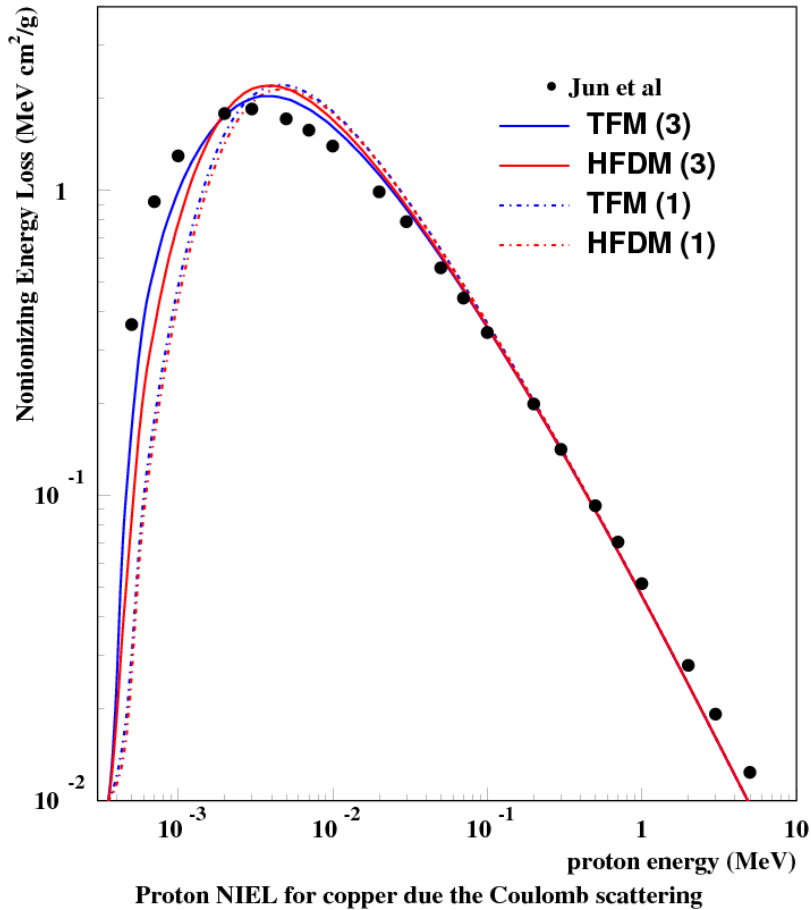
Atomic displacement cross sections obtained using MARS post-NRT models and BCA-MD IOTA calculations are close to each other and experimental data at proton energies $< 50 - 100$ MeV. This energy range cover needs of most applications.

To enhance reliability of MARS prediction at high energy, defect efficiency for large damage energies (> 100 keV) should be studied using MD-BCA approach. Post-NRT corrections should be improved in this energy range.

BACKUP

Full form factor against Moliere approximation

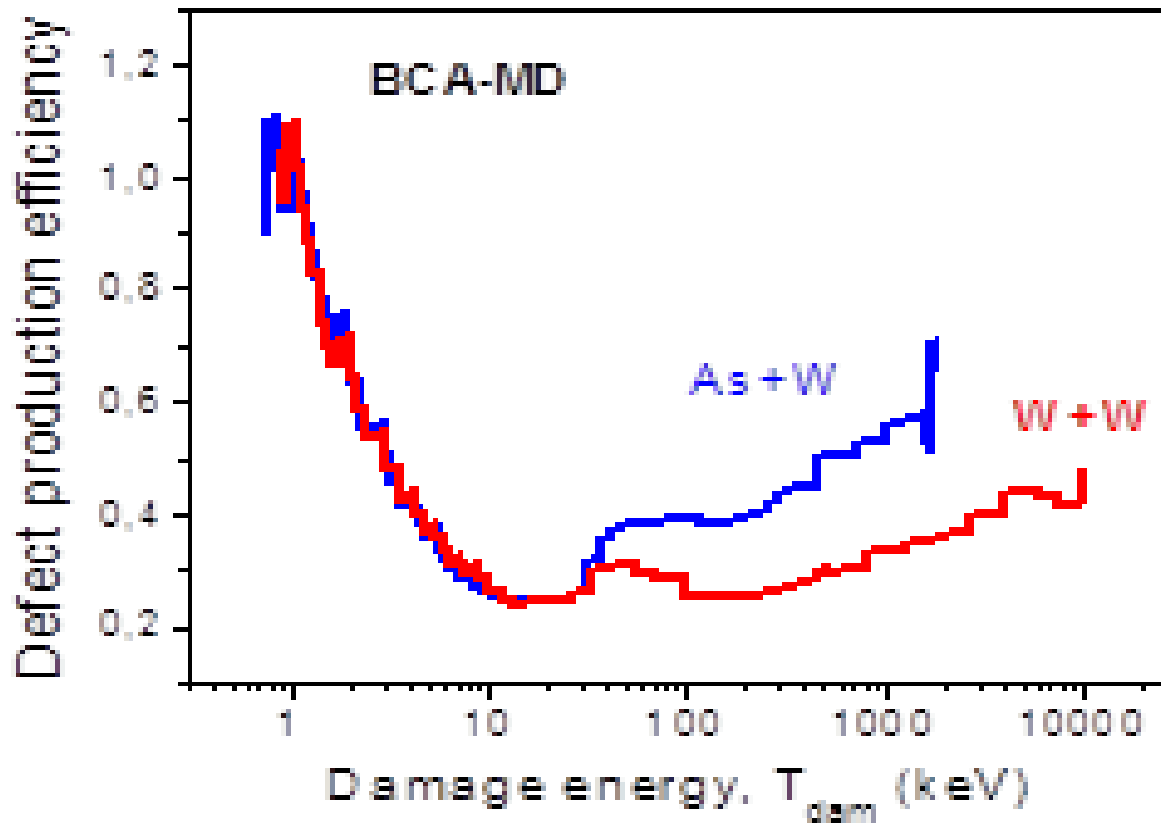
Jun(25eV) < IOTA(30eV)?
Different atomic screening?



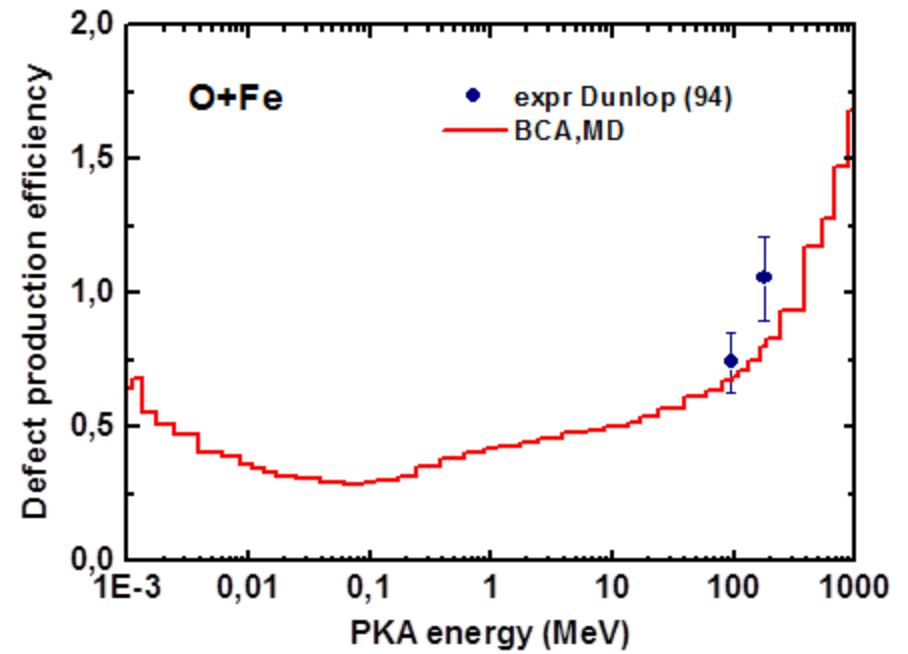
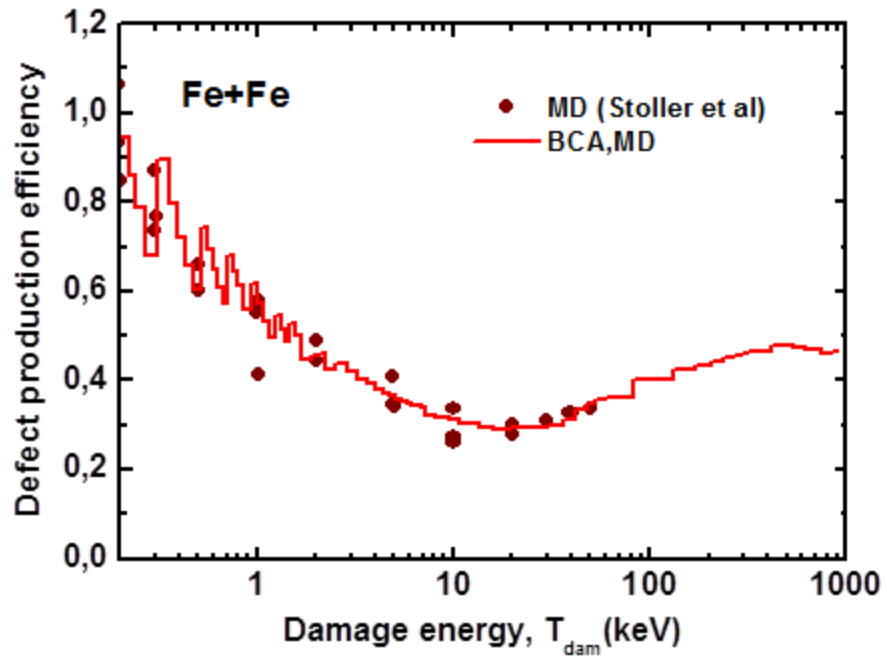
ERM - electrical resistivity measurement, ERMS - ERM on single crystals,
LPM - lattice parameter measurement, HS - Huang scattering

Metal	ρ_F [$\mu\Omega\text{m/u.c.}$]	Method	Ref.	Metal	ρ_F [$\mu\Omega\text{m/u.c.}$]	Method	Ref.
Mg	≥ 0.8	ERM	69 F	Tb	155 ± 30	ERM	80 D 1
	4.5	ERM	72 O	Th	15	ERM	73 G 2
	4 ¹⁾	ERM	75 L 1		(19) ¹⁾	ERM	75 L 1
	<u>9</u>	HS-LPM/ERM	82 E 1	Ti	18	ERM	72 S 1
Mo	4.5	ERM	62 L 1		(10) ¹⁾	ERM	75 L 1
	10	ERM	73 R	Tm	140 ± 30	ERM	80 D 1
	13 ± 2	ERM-S	75 M 5	U	22	ERM + LPM	87 W
	15 ± 4	HS-LPM/ERM	78 E	V	5.2...7.5	ERM	75 C 1
Nb	<u>16</u>	ERM	75 L 1		21.6 ²⁾	ERM	80 J
	14 ± 3	HS-LPM/ERM	78 E		22 ± 7 ²⁾	ERM	85 D 3
Nd	135 ± 35	ERM	85 D 1	W	7.5...16.0	ERM-S	78 M
Ni	6	ERM	75 L 1		14	ERM	75 L 1
	7.1 ± 0.8	HS-LPM/ERM	83 B		28	ERM	80 K
Pb	≤ 1	ERM	74 B 2		27 ± 6 ²⁾	ERM	85 D 3
	20	ERM	75 L 1	Y	50 ± 20	ERM	80 D 2
Pd	9 ± 1	ERM	67 J	Yb	75 ± 25	ERM	80 D 2
	9.2 ± 0.5 ²⁾	ERM	85 D 3	Zn	5	ERM	71 M 2
Pr	135 ± 35	ERM	85 D 1		4.2 ± 5	ERM	73 M 4
Pt	9.5 ± 0.5	ERM-S	73 J 2		20 ± 3	ERM-S	73 M 2
Re	<u>20</u>	ERM	74 V 1		15 ± 5	ERM-S	77 v
Sc	50	ERM	85 D 4		15 ± 5	HS-LPM/ERM	78 E
Sm	140 ± 30	ERM	80 D 2		15.3	HS-LPM/ERM	79 E 2
Sn (β)	1.1 ± 0.2	ERM	75 M 1	Zr	35.0	ERM	70 N
	4 ± 2 ²⁾	ERM	85 D 3		40	ERM	71 B 2
Ta	17 ± 3	ERM-S	72 J		35 ± 8	HS-LPM/ERM	82 E 1
	16 ± 3	ERM-S	79 B 3				

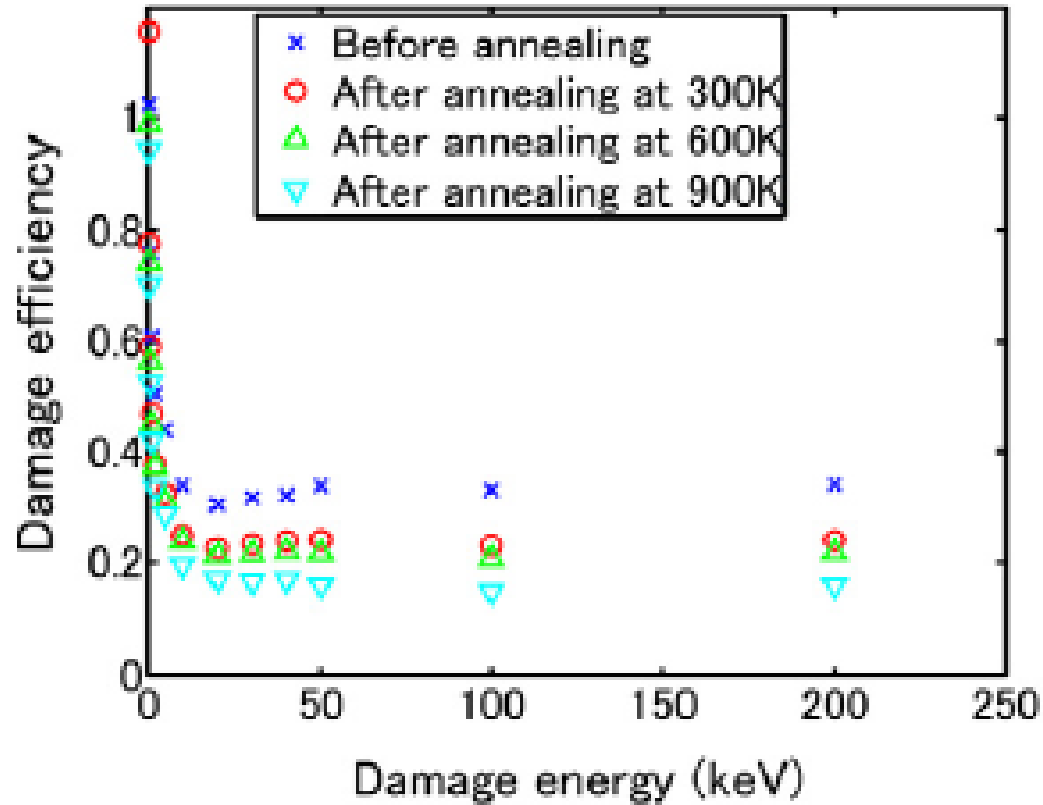
Combined BCA-MD simulations



Combined BCA-MD simulations



Kinetic Monte Carlo simulations - up to 10^4 s



KMC vs MD

